

Carlos Escande,^{1,2,3} Veronica Nin,^{1,2} Tamar Pirtskhalava,¹ Claudia C.S. Chini,^{1,2} Tamar Tchkonja,¹ James L. Kirkland,¹ and Eduardo N. Chini^{1,2}



Deleted in Breast Cancer 1 Limits Adipose Tissue Fat Accumulation and Plays a Key Role in the Development of Metabolic Syndrome Phenotype

Diabetes 2015;64:12–22 | DOI: 10.2337/db14-0192

Obesity is often regarded as the primary cause of metabolic syndrome. However, many lines of evidence suggest that obesity may develop as a protective mechanism against tissue damage during caloric surplus and that it is only when the maximum fat accumulation capacity is reached and fatty acid spillover occurs into peripheral tissues that metabolic diseases develop. In this regard, identifying the molecular mechanisms that modulate adipocyte fat accumulation and fatty acid spillover is imperative. Here we identify the deleted in breast cancer 1 (DBC1) protein as a key regulator of fat storage capacity of adipocytes. We found that knockout (KO) of DBC1 facilitated fat cell differentiation and lipid accumulation and increased fat storage capacity of adipocytes in vitro and in vivo. This effect resulted in a “healthy obesity” phenotype. DBC1 KO mice fed a high-fat diet, although obese, remained insulin sensitive, had lower free fatty acid in plasma, were protected against atherosclerosis and liver steatosis, and lived longer. We propose that DBC1 is part of the molecular machinery that regulates fat storage capacity in adipocytes and participates in the “turn-off” switch that limits adipocyte fat accumulation and leads to fat spillover into peripheral tissues, leading to the deleterious effects of caloric surplus.

Metabolic syndrome constitutes a leading cause of death in the world (1). Several conditions, including type 2 diabetes, liver steatosis, cardiovascular disease, stroke, dementia, and cancer, are believed to be modulated by the

metabolic dysfunction encountered in metabolic syndrome (2). Obesity has been proposed to be a component or a risk factor for metabolic syndrome and many other human conditions. Fat tissue can be the largest organ in the body (3), and its function has a crucial role in the physiology of the entire organism (3).

Although obesity is commonly seen as a cause of metabolic dysfunction, experimental evidence supports the notion that, in the context of caloric surplus, individuals may be protected against the development of metabolic dysfunction as long as they maintain functional adipocyte fat storage capacity and low levels of fat tissue inflammation (4). Once fat storage capacity is surpassed or fat tissue becomes dysfunctional, fatty acid spillover occurs, leading to ectopic fat accumulation in peripheral tissues and lipotoxicity, and eventually, systemic metabolic disease (5,6). In fact, it has been proposed that obesity is protective against metabolic diseases until fat accumulation capacity is reached and fatty acid spillover begins (4,7). Several lines of evidence support this idea: First, lipodystrophic humans and animals are highly susceptible to the development of insulin resistance, liver steatosis, and cardiac diseases (8,9). Second, an increase in adipocyte storage capacity, such as overexpression of adiponectin in *ob/ob* mice and overexpression of PEPCK in fat tissue, leads to an increase in weight and fat gain under high-caloric feeding but preservation of insulin sensitivity and metabolic health (10,11). Finally, it has been

¹Kogod Aging Center, Mayo Clinic, Rochester, MN

²Department of Anesthesiology, Mayo Clinic, Rochester, MN

³Institut Pasteur Montevideo, Montevideo, Uruguay

Corresponding author: Eduardo N. Chini, chini.eduardo@mayo.edu.

Received 3 February 2014 and accepted 17 July 2014.

This article contains Supplementary Data online at <http://diabetes.diabetesjournals.org/lookup/suppl/doi:10.2337/db14-0192/-/DC1>.

© 2015 by the American Diabetes Association. Readers may use this article as long as the work is properly cited, the use is educational and not for profit, and the work is not altered.

observed in humans that obesity may be protective against metabolic syndrome as long as fat accumulation occurs preferentially in subcutaneous fat (12,13). In fact, fatty acid spillover had been shown to inversely correlate with obesity in diabetic subjects (7). Because adipocyte fat accumulation and obesity can delay the development of metabolic diseases, it is key to identify the molecular pathways that are involved in the “turn on-off” switch that limits adipose tissue fat storage capacity and can modulate fatty acid spillover and the development of metabolic dysfunction.

In recent years, we have been studying the role of the deleted in breast cancer 1 (DBC1) protein. DBC1 binds and regulates many nuclear proteins, including SIRT1 (14–16), HDAC3 (17), Rev-erba (18), ER- α (19) and ER- β (20), BRCA1 (21), SUV39H1 (22), and IKK- β (23). We were the first to show that DBC1 is a SIRT1 inhibitor *in vivo* and that DBC1 plays a key role in metabolism (15). DBC1 knockout (KO) mice are protected against liver steatosis and nonalcoholic steatohepatitis (15). On the basis of our findings, we proposed that DBC1 might constitute a key regulator of metabolism during metabolic disorders.

Here we describe the role of DBC1 in the development of fat tissue dysfunction and the development of metabolic diseases during caloric surplus. We found that DBC1 KO mice become more obese than their wild-type (WT) litter mates when fed a high-fat diet. Interestingly, we found that despite being more obese, DBC1 KO mice had low free fatty acid (FFA) levels in blood, preserved insulin sensitivity, less atherosclerosis, less liver steatosis, and lived longer during high-fat diet feeding compared with their WT litter mates. Furthermore, we found preserved adipocyte fat storage capacity in DBC1 KO mice under caloric surplus. We propose that DBC1 modulates fat tissue function, fat accumulation, fatty acid spillover, and peripheral tissue damage. We propose that DBC1 is a key molecular component of the “on-off” switch that controls total adipocyte fat accumulation and fat tissue function and links obesity to its deleterious metabolic effects. Manipulation of this pathway may help prevent the negative effect of caloric surplus and obesity in health.

RESEARCH DESIGN AND METHODS

Reagents and Antibodies

Unless otherwise specified, all reagents and chemicals were purchased from Sigma-Aldrich. Antibodies purchased were SIRT1, vascular cell adhesion molecule (VCAM)-1, and activated caspase 3 (Cell Signaling Technology), PEPCK (Cayman Chemical Company), F4/80 (Abcam), DBC1 (Bethyl Laboratories), p53 and p21 (Santa Cruz Biotechnology, Inc.), and actin (Sigma-Aldrich). Human aortic endothelial cells and EGM2 culture media were purchased from Lonza.

Animal Handling and Experiments

The mice used in this study were females and were maintained in the Mayo Clinic Animal Breeding facility.

All experimental protocols were approved by the Mayo Clinic Institutional Animal Care and Use Committee. For the metabolic studies, mice were fed *ad libitum* a normal control diet (diet No. 3807; KLIBA-NAFAG), a high-fat diet (AIN-93G, modified to provide 60% of calories from fat; Dyets, Inc.), or a Western diet (TD.88137; 42% fat, 0.2% cholesterol; Harlan Laboratories). Body weight was recorded weekly. Food intake was measured for 7 consecutive days, with no difference detected between groups. Fat accumulation was measured by MRI (EcoMRI; EchoMedical Systems, Houston, TX) or by microcomputed tomography (micro-CT) scan (vivaCT40; SCANCO Medical, Zurich, Switzerland). For insulin tolerance testing, mice were food starved for 6 h before receiving a single intraperitoneal insulin injection (0.5 units/kg). Glycemia was measured from the tail vein. For survival experiments, mice were fed the normal chow diet until 6 months of age and were switched to the high-fat diet. Kaplan-Meier curves were generated using more than 20 mice per group. In all experiments, only litter mates were used.

Preadipocyte Culture and Differentiation

Fat depots were removed under sterile conditions. Fat tissue was minced into fragments, digested with 1 mg/mL type II collagenase (Worthington Biochemical Corp.) for 60 min at 37°C, and filtered through a 100- μ m nylon mesh. After digestion, mature adipocytes were separated from stromal vascular cells by centrifugation at 1,000g for 10 min. The pellets were resuspended in α -minimum essential medium containing 10% calf serum and antibiotics. Cells were placed in a humidified incubator (3% oxygen). After 16 h, adherent preadipocytes were replated at a density of 5×10^4 cells/cm².

To induce differentiation, subconfluent preadipocytes were exposed to differentiation medium containing DMEM/F12, 10% FBS, 1 μ g/mL insulin, 250 nmol/L dexamethasone, 0.5 mmol/L isobutylmethylxanthine, and 2.5 μ mol/L rosiglitazone in 5% oxygen. After 48 h, all ingredients except insulin and FBS were removed from the medium. Cells were differentiated for 5–10 days.

Immunoprecipitation and Western Blotting

Mouse tissues and cultured cells were lysed in NETN buffer (20 mmol/L Tris-HCl, pH 8.0; 100 mmol/L NaCl; 1 mmol/L EDTA; and 0.5% NP-40) supplemented with 5 mmol/L NaF, 50 mmol/L 2-glycerophosphate, and a protease inhibitor cocktail (Roche Diagnostics). For each immunoprecipitation, 1 mg protein was used.

SIRT1 Activity Measurement

SIRT1 activity was measured from SIRT1 immunoprecipitates from tissue as previously described (15).

Atherosclerosis Model

Mice were fed the Western-style diet starting at 8 weeks of age. After 8–20 weeks of the diet, the aorta was dissected to the iliac bifurcation, opened longitudinally, and pinned in place on black wax. Lipid-rich regions were

stained with Oil Red O. Image analysis was performed using ImageJ software (National Institutes of Health). Lesion area was calculated for each animal as a percentage of the total aortic area, and the lesion number was expressed as plaques per aorta. All quantifications were performed blindly by independent personnel.

Ex Vivo Glycerol Production in Fat Tissue

The method used to measure glycerol production by adipose tissue in vitro was a modification of a method described by Vaughan (24). Inguinal fat pads (50–75 mg) were incubated for 2 h at 37°C in 3 mL Krebs-Ringer bicarbonate HEPES buffer (pH 7.4), containing 3% BSA (fatty acid-free) and 5 mmol/L pyruvate. Glycerol levels were analyzed in the medium before and after the incubation using a glycerol determination kit (Cayman Chemical Company). Glycerol production from external pyruvate was calculated by comparing glycerol levels in the media after 2 h incubation, with or without 5 mmol/L pyruvate, for each fat depot.

Determination of Metabolically Relevant Molecules in Plasma

The following molecules were assayed in plasma from mice after starvation for 6 h: triglycerides (Infinity; Thermo Scientific), cholesterol (CardioChek; Chek Diagnostics),

insulin (BD Biosciences), glycerol (Cayman Chemical Company), and adiponectin (R&D Biosystems).

Cell and Fat Tissue Coculture

Human aortic endothelial cells were plated with coverslips. The next day, inguinal fat tissue was dissected under sterile conditions. Tissue (1 g) was cut into small pieces and put in six-well plates. Tissue was incubated in the media before the cells were added. Coverslips with attached cells were placed into a ThinCert chamber (0.4- μ m pore size; Greiner Bio-One) and put inside the well with fat tissue. After overnight incubation, cells were fixed with 4% paraformaldehyde and further processed for standard immunofluorescence.

Statistics

Values are presented as mean \pm SEM of three to five experiments, unless otherwise indicated. The significance of differences between means was assessed by ANOVA or a two-tailed Student *t* test, as indicated. A *P* value of <0.05 was considered significant.

RESULTS

High-Fat Diet Promotes SIRT1-DBC1 Interaction and Decreases SIRT1 Activity in Fat Tissue

In previous work, we showed that DBC1 plays a key role in metabolism by regulating SIRT1 activity and function

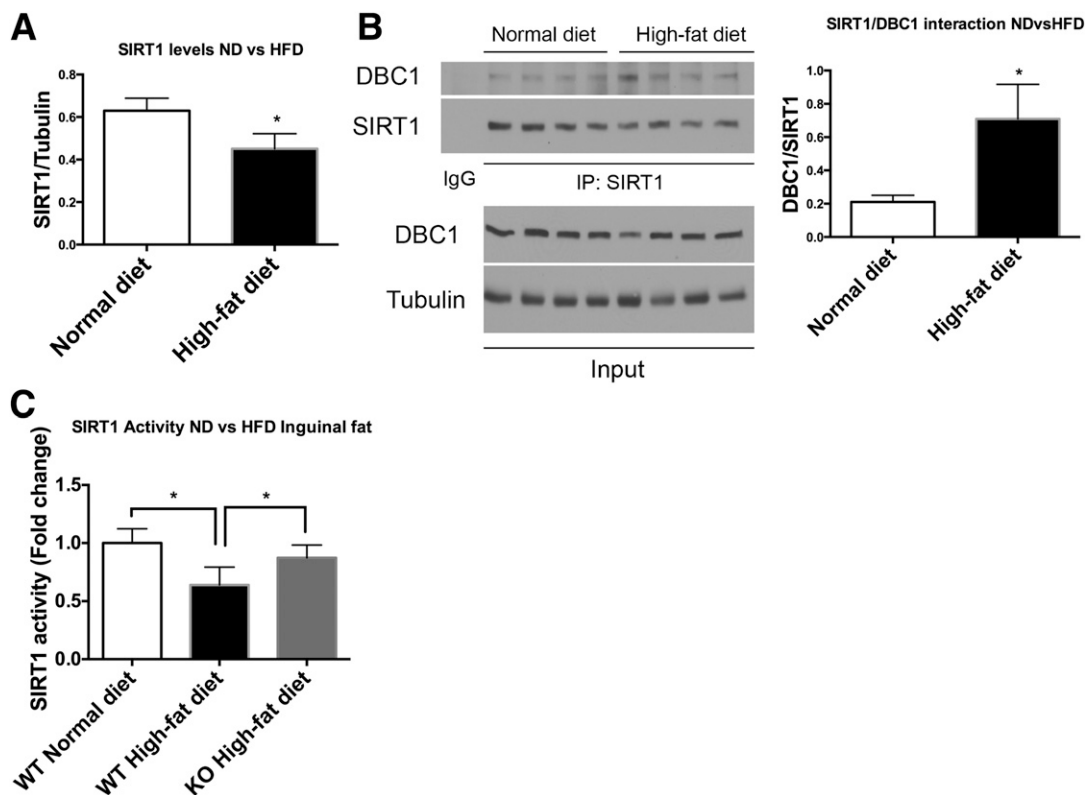


Figure 1—High-fat diet (HFD) feeding promotes SIRT1/DBC1 interaction and decreases SIRT1 activity in fat tissue. **A**: SIRT1 levels in inguinal fat tissue from 6-month-old mice fed the normal chow diet (ND) or the HFD for 20 weeks ($n = 5$ mice per group). $*P < 0.05$. **B**: Representative Western blot (left) of coimmunoprecipitation between SIRT1 and DBC1 in fat tissue from mice fed the ND or HFD, with each lane corresponding to a different mouse, and quantitation (right) of SIRT1/DBC1 interaction by densitometry ($n = 4$ mice per group). $*P < 0.05$. **C**: SIRT1 activity from immunoprecipitates of inguinal fat tissue in mice in fed the ND or HFD ($n = 5$ mice per group). $*P < 0.05$.

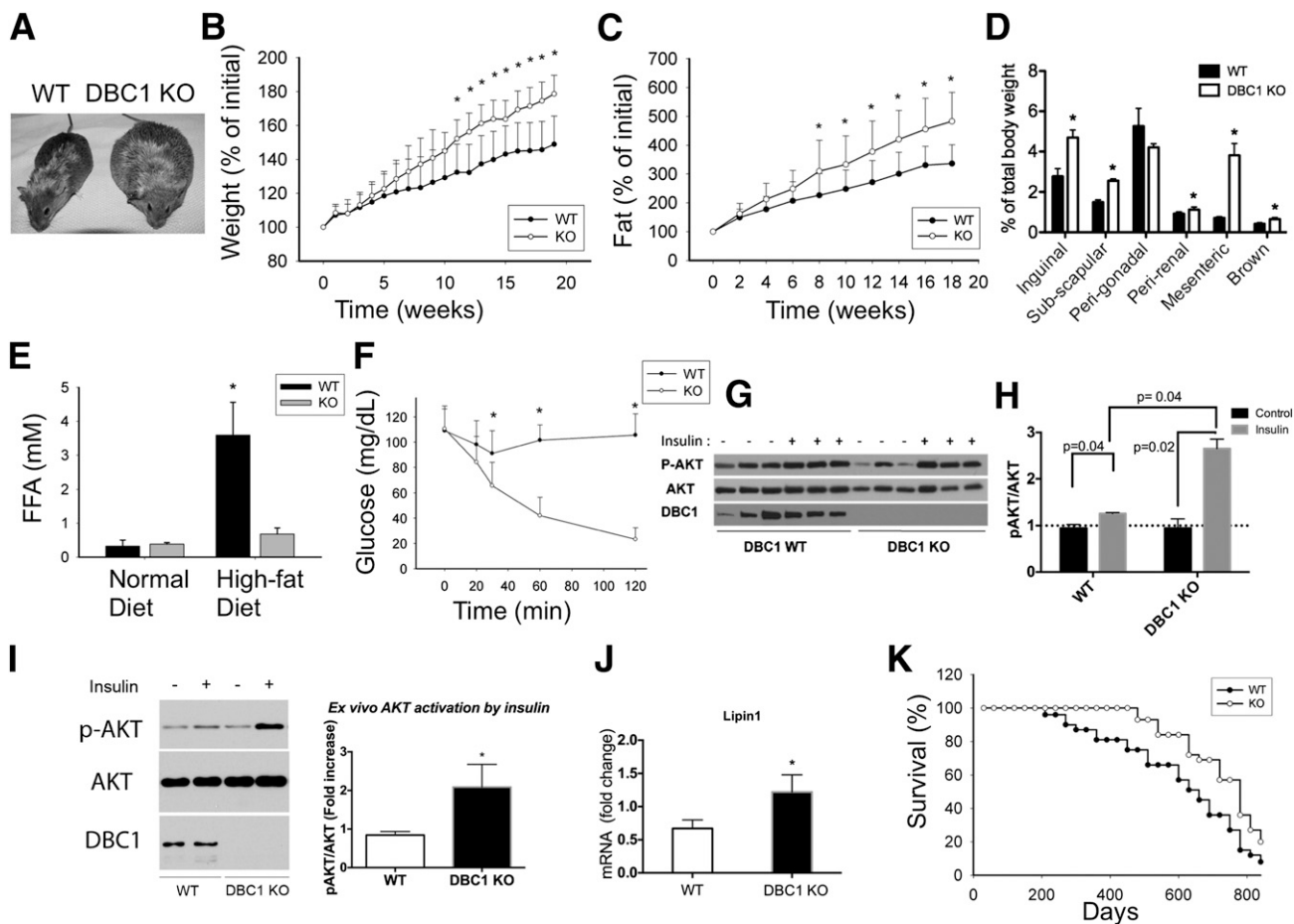


Figure 2—Deletion of DBC1 in vivo increases fat tissue accumulation capacity and prevents FFA spill over, protecting against insulin resistance. *A*: Representative photograph of WT (left) and DBC1 KO (right) siblings at 6 months of age and after 4 weeks of being fed the high-fat diet. *B*: Weight gain of WT and DBC1 KO mice fed the high-fat diet. The mice were switched from regular breeding chow to the high-fat diet starting at 6 months of age. Weight gain was monitored periodically during the treatment ($n = 16$ mice per group). $*P < 0.05$. *C*: Fat accumulation in the same mice described in *B*. Fat content in vivo was measured by MRI scanning ($n = 16$ mice per group). $*P < 0.05$. *D*: Quantification of different fat depots in WT and DBC1 KO mice after being fed the high-fat diet for 12 weeks. Fat tissue weight was expressed, corrected by total body weight ($n = 5$ mice per group). $*P < 0.05$. *E*: FFA levels in blood in WT and DBC1 KO adult mice fed regular breeding chow or after 12 weeks of the high-fat diet ($n = 8$ mice per group). $*P < 0.05$. *F*: Insulin tolerance test in WT and DBC1 mice fed the high-fat diet for 12 weeks. After 6 h of food starvation, mice were challenged with 0.5 units/kg of intraperitoneal insulin, and glycemia was monitored over time ($n = 8$ mice per group). $*P < 0.05$. *G*: Western blot shows phosphorylation of AKT (p-AKT) in inguinal fat tissue after WT and DBC1 KO mice fed the high-fat diet were challenged with 0.5 units/kg insulin for 15 min. *H*: Band intensity was measured by densitometry and expressed as the ratio of p-AKT to total AKT. *I*: Ex vivo insulin sensitivity in fat tissue from WT and DBC1 KO mice after 12 weeks of being fed the high-fat diet. Inguinal fat was incubated in Krebs-Ringer buffer with 5 mU/L insulin for 15 min. Tissue was later processed for Western blotting. *Left*, Representative Western blot of p-AKT after incubation with insulin. *Right*, Quantitation of p-AKT after insulin treatment expressed as the fold increase over control (no treatment) ($n = 5$ mice per group). $*P < 0.05$. *J*: Expression of lipin1 mRNA in inguinal fat tissue of WT and DBC1 KO after 12 weeks of the high-fat diet ($n = 4$). $*P < 0.05$. *K*: Survival curve of WT and DBC1 KO mice fed standard chow until 6 months of age and then fed the high-fat diet ($n = 22$ mice per group).

(15) and further found that a high-fat diet promotes SIRT1-DBC1 interaction and decreases SIRT1 activity in the liver. Here, we investigated whether DBC1 plays an active role in adipocyte and fat tissue function. We found that the high-fat diet leads to a decrease in SIRT1 expression in fat tissue (Fig. 1A) and that the data are consistent with previously published data (25). Interestingly, we found an increase in SIRT1 binding to DBC1 during the high-fat diet (Fig. 1B), with a consequent decrease in SIRT1 activity (Fig. 1C). The decrease in SIRT1 activity

in the fat tissue induced by the high-fat diet was prevented by deletion of DBC1 (Fig. 1C). These results suggested to us that DBC1 regulates SIRT1 activity in fat tissue during fat and caloric surplus and that DBC1 KO mice may be protected against fat tissue dysfunction induced by caloric surplus. Our findings that SIRT1 regulation by DBC1 during obesity may not be reflected during aging is worth noting: the expression of both SIRT1 and DBC1 decreases (Supplementary Fig. 1A) during aging, suggesting a different mechanism of regulation.

DBC1 KO In Vivo Promotes Increases in Adipocyte Fat Accumulation Capacity, Prevents FFA Spillover, and Protects Against Insulin Resistance

We fed adult WT and DBC1 KO female mice the high-fat diet for 20 weeks and observed that the DBC1 KO mice gained more weight than their WT litter mates. This trend was constant during the entire duration of the study and became statistically significant after 12 weeks of the high-fat diet (Fig. 2A and B). We observed the same trend when we measured fat accumulation by MRI (Fig. 2C). The post-mortem analysis of different fat depots showed a significant increase in inguinal, subscapular, mesenteric, perirenal, and brown fat (Fig. 2D). There were no significant changes in the total amount of perigonadal fat between WT and DBC1 KO mice when corrected by total body weight (Fig. 2D). Interestingly, we found that despite being more obese, DBC1 KO mice fed the high-fat diet had FFA levels that resembled those measured in mice fed the normal chow diet (Fig. 2E) and that they were also protected against fatty liver disease (Supplementary Fig. 1B). This was paralleled by protection against insulin resistance. We found that DBC1 KO mice were more sensitive to an insulin challenge by performing insulin tolerance test (Fig. 2F) and that AKT phosphorylation was increased in fat tissue in vivo after the mice were challenged with a dose of insulin (Fig. 2G and H). Also, AKT phosphorylation was increased in skeletal muscle in DBC1 KO mice (Supplementary Fig. 2A). Moreover, we found that DBC1 deletion preserves insulin sensitivity in fat by an ex vivo challenge with insulin (Fig. 2I), suggesting that DBC1 KO mice were preserving insulin sensitivity by preventing fat tissue dysfunction. Consistent with the increased fat accumulation and protection against insulin resistance, we found that lipin1 mRNA levels were increased in fat tissue from DBC1 KO mice (Fig. 2J). Lipin1 promotes fatty acid esterification, and its expression has been linked to insulin sensitivity and healthy fat accumulation in mice and humans (26,27).

We also monitored the longevity of WT and DBC1 KO mice fed the high-fat diet starting at 6 months of age and found that the DBC1 mice had an increased median life span, although the maximal life span was not significantly extended (Fig. 2K). Worth noticing, we found that increased fat accumulation and protection against fatty acid spillover was not restricted to mice fed the high-fat diet but also happened in old adult mice fed the normal chow diet their entire life. DBC1 KO mice that were 14 months old were heavier (Fig. 3A), had increased whole-body fat content (Fig. 3B), decreased FFA in plasma (Fig. 3C), and lower glucose levels in plasma (Fig. 3D) than their WT litter mates.

DBC1 KO Improves Fat Differentiation Capacity in Preadipocytes From Mice During Normal and High-Fat Diet Feeding

Next, we investigated if KO of DBC1 increases the fat differentiation potential of preadipocytes in mice. We purified and cultured preadipocytes from WT and DBC1

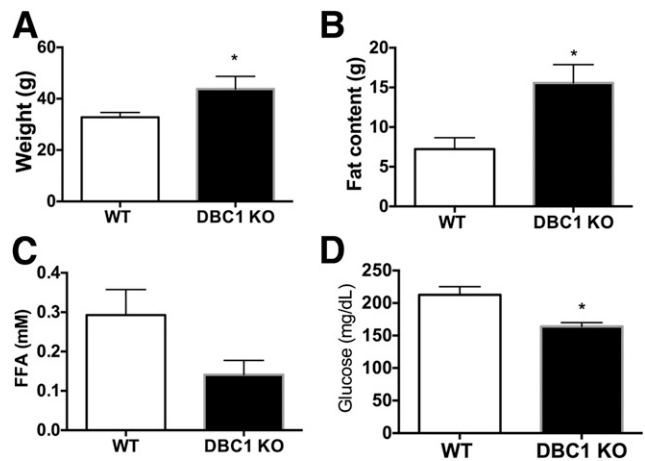


Figure 3—Deletion of DBC1 in vivo also prevents FFA spillover in old mice fed the normal chow diet. Weight (A), total body fat content measured by MRI (B), FFA in plasma (C), and glycemia (D) in 14-month-old mice fed the normal chow diet their entire life ($n = 4$ mice per group). * $P < 0.05$.

KO mice and found that DBC1 KO increases the differentiation potential of preadipocytes (Fig. 4A). Interestingly, this potential was also preserved during obesity. DBC1 KO increased the differentiation capacity in primary preadipocytes purified from the inguinal fat depot (Fig. 4B and C) and also from the epididymal fat depot (Fig. 4B and D) after 20 weeks of high-fat diet feeding. DBC1 KO in mice facilitates fat accumulation in fat tissue during obesity, which correlates with decreased FFA levels in plasma (Fig. 2). Because an increase in fat accumulation capacity could arise from increased lipid synthesis and esterification or from decreased lipolysis, we checked for lipolysis in vitro. Neither the main lipases (adipose triglyceride lipase and hormone-sensitive lipase) nor caveolin 1, another protein involved in lipolysis, were expressed differentially between WT and DBC1 KO differentiated adipocytes (Fig. 4E). Furthermore, we measured in vitro lipolysis in response to isobutylmethylxanthine in differentiated adipocytes and found no difference between WT and DBC1 KO cells (Fig. 4F).

ApoE^{-/-} DBC1^{-/-} Mice Have Increased Adipocyte Fat Accumulation Capacity and Decreased Inflammation in Fat Tissue

Cardiovascular diseases constitute the leading cause of death in adults, and there is a strong correlation between fat tissue dysfunction and cardiovascular morbidity. We investigated whether increased adipocyte fat storage capacity and a decrease in fatty acid spillover observed in the DBC1 KO mice could protect against cardiovascular dysfunction. For this, we crossed DBC1 KO mice with ApoE KO mice, to generate DBC1^{+/+}ApoE^{-/-} and DBC1^{-/-}ApoE^{-/-} mice. Pups from the different genotypes were obtained at Mendelian ratios, and there were no obvious phenotypic differences between genotypes. The ApoE KO mice are of particular value for these experiments because the atherosclerotic

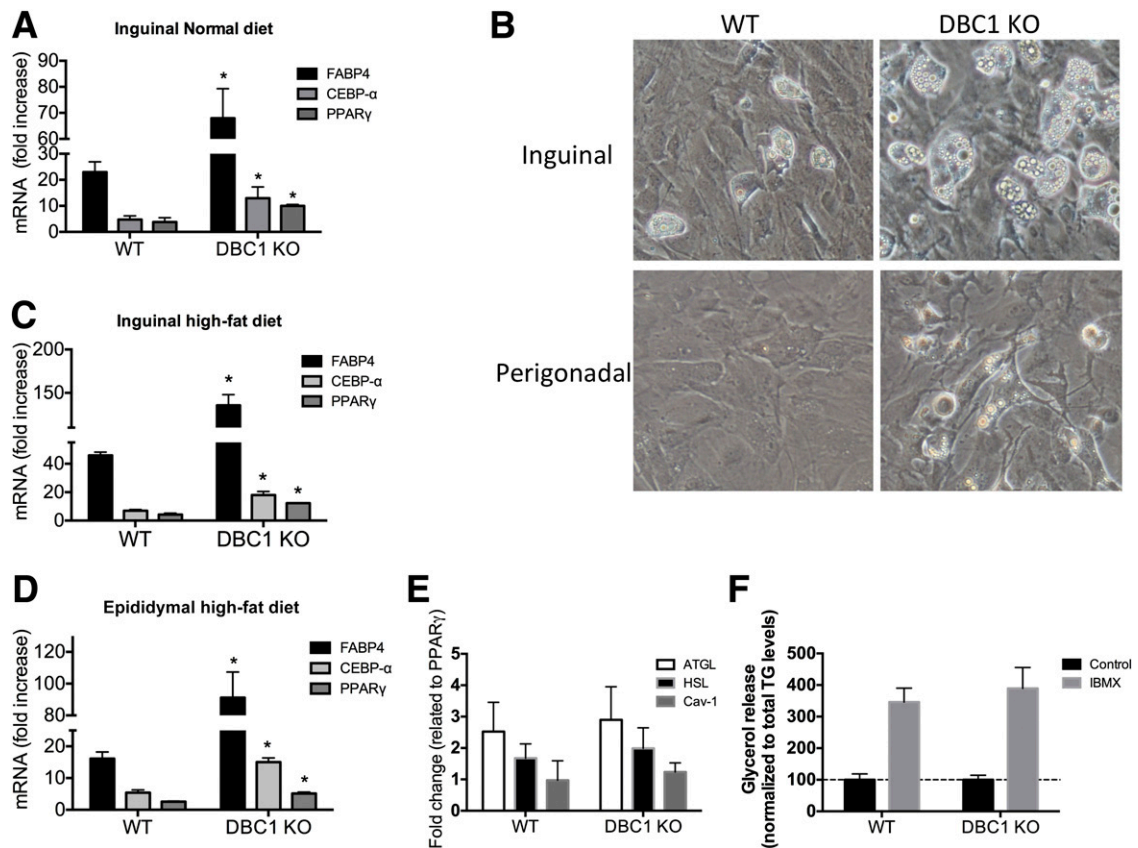


Figure 4—DBC1 KO increases fat differentiation capacity in preadipocytes isolated from mice fed the normal or high-fat diet. **A:** Gene expression analysis of adipogenesis markers by RT-PCR in inguinal preadipocytes isolated from mice fed the normal diet and after 5 days of differentiation ($n = 4$ mice per condition). $*P < 0.05$, t test. **B:** Representative image of differentiated primary adipocytes obtained from inguinal (upper panels) and perigonadal (lower panels) fat depots from WT and DBC1 KO mice. Cells were allowed to differentiate for 5 days after the addition of differentiation media. **C:** Gene expression analysis of adipogenesis markers by RT-PCR in inguinal (C) and perigonadal (D) mouse preadipocytes isolated from mice fed the high-fat diet and after 5 days of differentiation ($n = 4$ mice per condition). $*P < 0.05$, t test. **E:** Gene expression analysis of lipolysis markers by RT-PCR in inguinal mouse preadipocytes isolated from mice and after 5 days of differentiation. Results were normalized to peroxisome proliferator-activated receptor- γ (PPAR- γ) expression to correct for the difference in differentiation potential. **F:** In vitro lipolysis stimulated by isobutylmethylxanthine (IBMX; 100 $\mu\text{mol/L}$) in differentiated adipocytes from WT and DBC1 KO mice. Cells were incubated with IBMX or vehicle for 6 h. Glycerol content was determined from the cell culture media. Results were normalized to the total triglycerides (TG) content in the plate.

phenotype is modulated by adipocyte function in these animals (28,29). At the age of 8 weeks, female mice were challenged with a Western diet (42% fat and 0.2% cholesterol) for 20 weeks to induce atherosclerosis. We found that ApoE $^{-/-}$ DBC1 $^{-/-}$ mice behaved very similar to what we had previously observed for DBC1 KO mice in fat accumulation and weight gain when fed the Western diet. In fact, the difference in weight and fat gain was even more striking between ApoE $^{-/-}$ DBC1 $^{+/+}$ and ApoE $^{-/-}$ DBC1 $^{-/-}$ mice (Fig. 5A), probably because ApoE $^{-/-}$ is required for fat cell differentiation (30). We performed micro-CT scans in the mice after 20 weeks of the Western diet and observed increased fat content in different fat depots, including subcutaneous, abdominal, and visceral (Fig. 5B). We found that ApoE $^{-/-}$ DBC1 $^{-/-}$ mice have decreased $\dot{V}O_2$, $\dot{V}CO_2$, and energy expenditure than the ApoE $^{-/-}$ DBC1 $^{+/+}$ mice when fed the high-fat diet, consistent with the difference in weight (Supplementary

Fig. 3). We did not detect any significant difference in cholesterol, triglycerides, or insulin levels after 20 weeks of the Western diet (Table 1). However, adiponectin levels were significantly higher in the ApoE $^{-/-}$ DBC1 $^{-/-}$ mice (Table 1).

Histological analysis of perigonadal and inguinal fat depots dissected from ApoE $^{-/-}$ DBC1 $^{+/+}$ and ApoE $^{-/-}$ DBC1 $^{-/-}$ mice after 20 weeks of being fed the Western diet showed a clear and significant difference in adipocyte cell size, with cells coming from ApoE $^{-/-}$ DBC1 $^{-/-}$ between 3- and 10-times larger than those analyzed from control mice (Fig. 5C and D). We hypothesized that increased FFA esterification capacity in fat cells in the absence of DBC1 explained the increased fat cell size. To be able to accumulate more fatty acids, fat cells have to esterify them into triglycerides, and for that, glycerol must be available. We performed an ex vivo experiment where pieces of inguinal fat tissue were incubated with pyruvate,

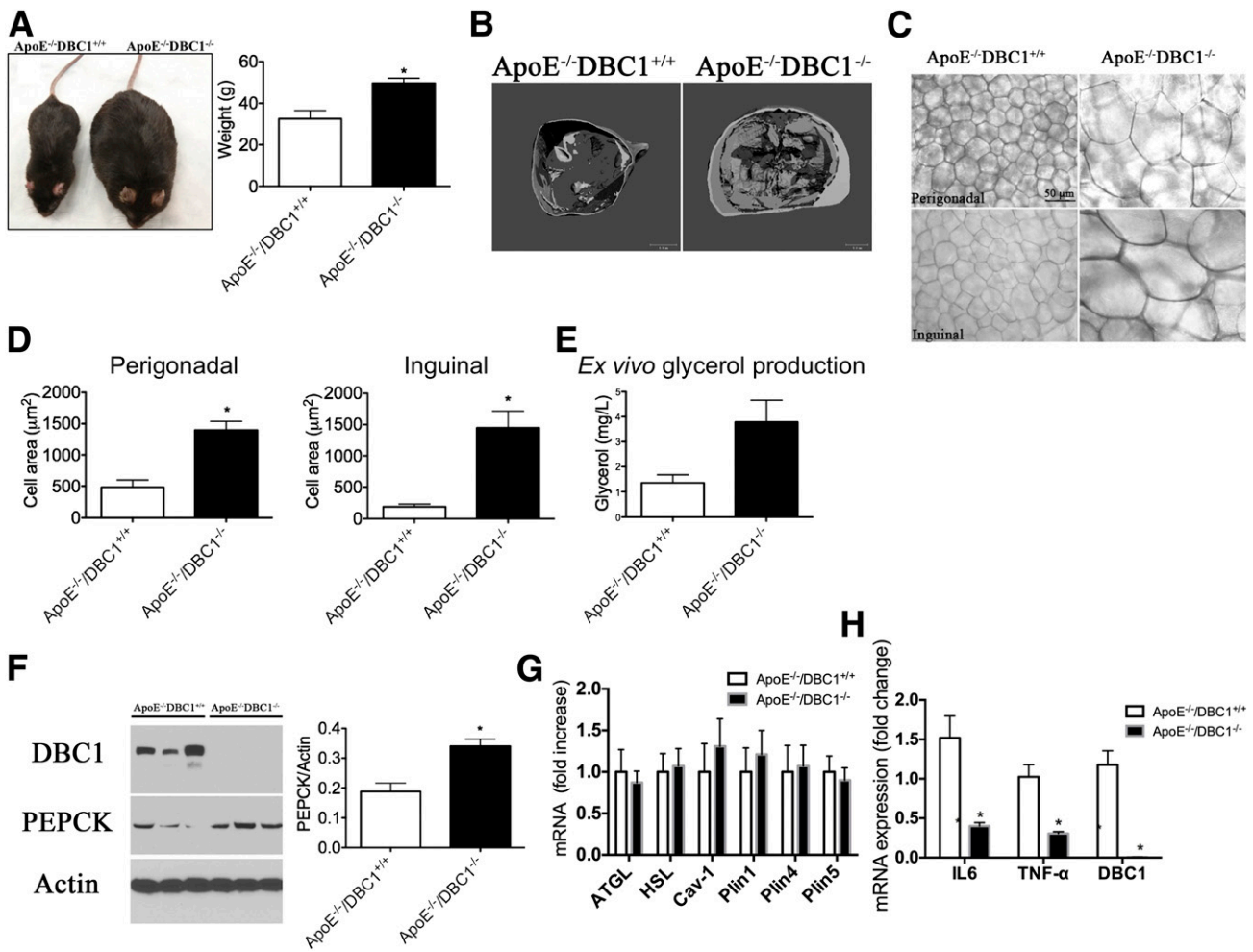


Figure 5—ApoE^{-/-} DBC1^{-/-} mice have increased fat accumulation capacity and decreased inflammation in fat tissue. **A: Left**, Representative photograph of ApoE^{-/-} DBC1^{+/+} (left side) and ApoE^{-/-} DBC1^{-/-} (right side) mice after 20 weeks of being fed the Western diet. **Right**, Weight of ApoE^{-/-} DBC1^{+/+} and ApoE^{-/-} DBC1^{-/-} mice at the end of the treatment with the Western diet ($n = 8$ per group). *Shows significant difference at $P < 0.05$, t test. **B**: Representative CT scan shows fat tissue content and distribution of adult ApoE^{-/-} DBC1^{+/+} and ApoE^{-/-} DBC1^{-/-} mice after 20 weeks of being fed the Western diet. **C**: Representative picture of fat cell size in perigonadal (upper panels) and inguinal (lower panels) fat depots dissected from ApoE^{-/-} DBC1^{+/+} and ApoE^{-/-} DBC1^{-/-} mice after 20 weeks of being fed the Western Diet. **D**: Fat cell size measurement in perigonadal (left) and inguinal (right) fat tissue depots of ApoE^{-/-} DBC1^{+/+} and ApoE^{-/-} DBC1^{-/-} mice after 20 weeks of being fed the Western diet ($n = 3$ per group). *Shows significant difference at $P < 0.05$, t test. **E**: Ex vivo glycerol production and release from inguinal fat tissue in response to pyruvate in mice after 5 weeks of being fed the Western diet ($n = 5$ per group). *Shows significant difference at $P < 0.05$, t test. **F**: PEPCK expression in the same mice and conditions described in **D** ($n = 3$ per group). *Shows significant difference at $P < 0.05$, t test. **G**: Gene expression analysis of lipolysis markers in inguinal fat tissue of ApoE^{-/-} DBC1^{+/+} and ApoE^{-/-} DBC1^{-/-} mice after 20 weeks of being fed the high-fat diet ($n = 6$ per group). **H**: Gene expression analysis of inflammation markers in inguinal fat tissue of ApoE^{-/-} DBC1^{+/+} and ApoE^{-/-} DBC1^{-/-} after 20 weeks of being fed the high-fat diet ($n = 5$ per group). *Shows significant difference at $P < 0.05$, t test.

and the production of glycerol (glyceroneogenesis) was measured. We found that fat tissue from ApoE^{-/-} DBC1^{-/-} mice had increased glyceroneogenesis capacity (Fig. 5E). Increased glyceroneogenesis was paralleled by increased expression of PEPCK (Fig. 5F), a key enzyme in this pathway. In fact, we previously described that DBC1 regulates gluconeogenesis and PEPCK expression in the liver (31). Interestingly, fat-specific overexpression of PEPCK promotes obesity and fat accumulation but also confers protection against insulin resistance (11), which is in agreement with our findings.

In agreement with our findings in cells in culture we found no difference in the lipolysis markers adipose triglyceride lipase, hormone-sensitive lipase, and caveolin 1 between ApoE^{-/-} DBC1^{+/+} and ApoE^{-/-} DBC1^{-/-} mice in adipose tissue (Fig. 5G). We also analyzed the expression of the lipid droplets coating proteins perilipin 1, 4, and 5 and found no difference in their expression levels between ApoE^{-/-} DBC1^{+/+} and ApoE^{-/-} DBC1^{-/-} mice (Fig. 5G). Finally, we found that increased fat storage capacity led to decreased expression of inflammation markers in fat tissue (Fig. 5H). The expression of tumor

Table 1—Triglycerides, insulin, adiponectin, and cholesterol levels in the plasma of ApoE^{-/-}DBC1^{+/+} and ApoE^{-/-}DBC1^{-/-} mice after 20 weeks of being fed the high-fat diet

	ApoE ^{-/-} DBC1 ^{+/+}		ApoE ^{-/-} DBC1 ^{-/-}	
	Average	SEM	Average	SEM
Cholesterol (mg/dL)	500		500	
Triglycerides (mg/dL)	776	213	784	150
Glycerol (mg/L)	56.8	9.3	80.3	12.0
Adiponectin (mg/L)*	9.84	0.42	14.63	0.92
Insulin (ng/mL)	0.16	0.05	0.40	0.13

*Shows significant difference, $P < 0.05$, t test ($n = 8$ per group).

necrosis factor- α and interleukin-6, two key inflammatory molecules involved in tissue dysfunction during obesity, was decreased in inguinal fat after the high-fat diet (Fig. 5H).

DBC1 KO Protects Mice Against Aortic Atherosclerosis, Inflammation, and Cellular and Tissue Damage

Finally, we determined the role of DBC1 in the development of atherosclerosis. We analyzed dissected aortas from ApoE^{-/-}DBC1^{+/+} and ApoE^{-/-}DBC1^{-/-} mice after 20 weeks of being fed the Western diet. Oil Red O staining of whole-mount aortas (Fig. 6A) showed a significant decrease in the total number of plaque formation (Fig. 6B) and in the total area with plaques (Fig. 6B) in ApoE^{-/-}DBC1^{-/-} compared with ApoE^{-/-}DBC1^{+/+} mice. We found a significant downregulation in the expression of several inflammation and damage markers at the mRNA level in the aortas of the ApoE^{-/-}DBC1^{-/-} compared with the ApoE^{-/-}DBC1^{+/+} mice. In particular, expression of p53, p21, p65, and MCP-1 were decreased in ApoE^{-/-}DBC1^{-/-} mice (Fig. 6C). Also, Western blot analysis from whole aortas showed decreased expression of markers of inflammation and tissue dysfunction such as VCAM-1, p53, and F4/80 (Fig. 6D). One of the early events in the development of atherosclerosis is the development of endothelial dysfunction (32). It has been proposed that FFAs play a role in the development of endothelial dysfunction and can cause endothelial apoptosis and endothelial insulin resistance (33).

To further investigate the mechanism by which DBC1 regulates the development of metabolic syndrome, we determine if prevention of fatty acid spillover induced by DBC1 KO protects against peripheral cell and tissue damage. In this regard, we performed coculture experiments with fat tissue and aortic endothelial cells in the presence of FFAs. Overnight incubation of aortic endothelial cells with 500 μ mol/L palmitate in the presence of inguinal fat obtained from ApoE^{-/-}DBC1^{+/+} mice led to cytotoxicity in endothelial cells and resulted in apoptosis. However, when the cells were cocultured with fat tissue obtained from ApoE^{-/-}DBC1^{+/+}, apoptosis in endothelial cells was significantly decreased (Fig. 6E and F). At the end of the experiment, we measured FFA levels in the

media and found that in the presence of fat coming from ApoE^{-/-}DBC1^{-/-} mice, FFA levels in the media were decreased, likely due to the increased fat buffering capacity from DBC1 KO adipocytes (Fig. 6G). In fact, as seen in our other experiments, ApoE^{-/-}DBC1^{-/-} mice also showed decreased FFA levels in plasma compared with ApoE^{-/-}DBC1^{+/+} controls (Fig. 6H). Taken together, our results indicate that DBC1 modulates fat tissue function, fatty acid spillover, and the development of features of metabolic syndrome.

DISCUSSION

Obesity-related systemic dysfunction, such as inflammation, insulin resistance, type 2 diabetes, liver steatosis, cardiovascular disease, and stroke, are among the leading causes of death in adults in Western countries (1), and only in the U.S. does obesity affect 35.7% of adults (1). Thus, understanding how obesity leads to tissue dysfunction is of key importance to the development of new therapeutic approaches.

Our work shows that DBC1 KO female mice are significantly more obese than their WT litter mates but remain “healthier” under a normal diet and also under diet-induced obesity. We propose that during obesity, metabolic diseases arise, at least in part, as a consequence of saturation of the storage capacity in fat tissue and spillover of fatty acids to the media, and we provide a new molecular pathway that links fat tissue dysfunction to metabolic syndrome. It is important to highlight that the phenotype of “healthy obesity” described in this work happens primarily in female adult mice but not in males. In fact, although male DBC1 KO mice tend to gain more weight than their WT litter mates, they do not differ in their insulin sensitivity when they are fed a high-fat diet, as we recently showed (31). This is an interesting point, because the “healthy obesity” phenotype observed in humans when there is increased subcutaneous fat deposition has been shown to happen primarily in women (34).

We recently showed that deletion of DBC1 protects against cellular senescence in adipose tissue during obesity (35). In fact, the absence of cellular senescence in DBC1 KO mice can be seen as another characteristic of the “healthy obesity” phenotype that we describe here, because it has been shown that obesity leads to an increase in cellular senescence in obese subjects (3). It would be interesting to determine whether individuals that display a healthy obesity phenotype also have protection against cellular senescence and also to determine whether there is any kind of change in the expression of DBC1 in these individuals. Our recent work also shows that the role of DBC1 in the regulation of cellular senescence in fat tissue might be restricted to high-caloric loads and not to aging, because we failed to see changes in senescence between WT and DBC1 KO during aging (35), although we could only study the mice until 18 months of age, and differences between mice might arise later in life.

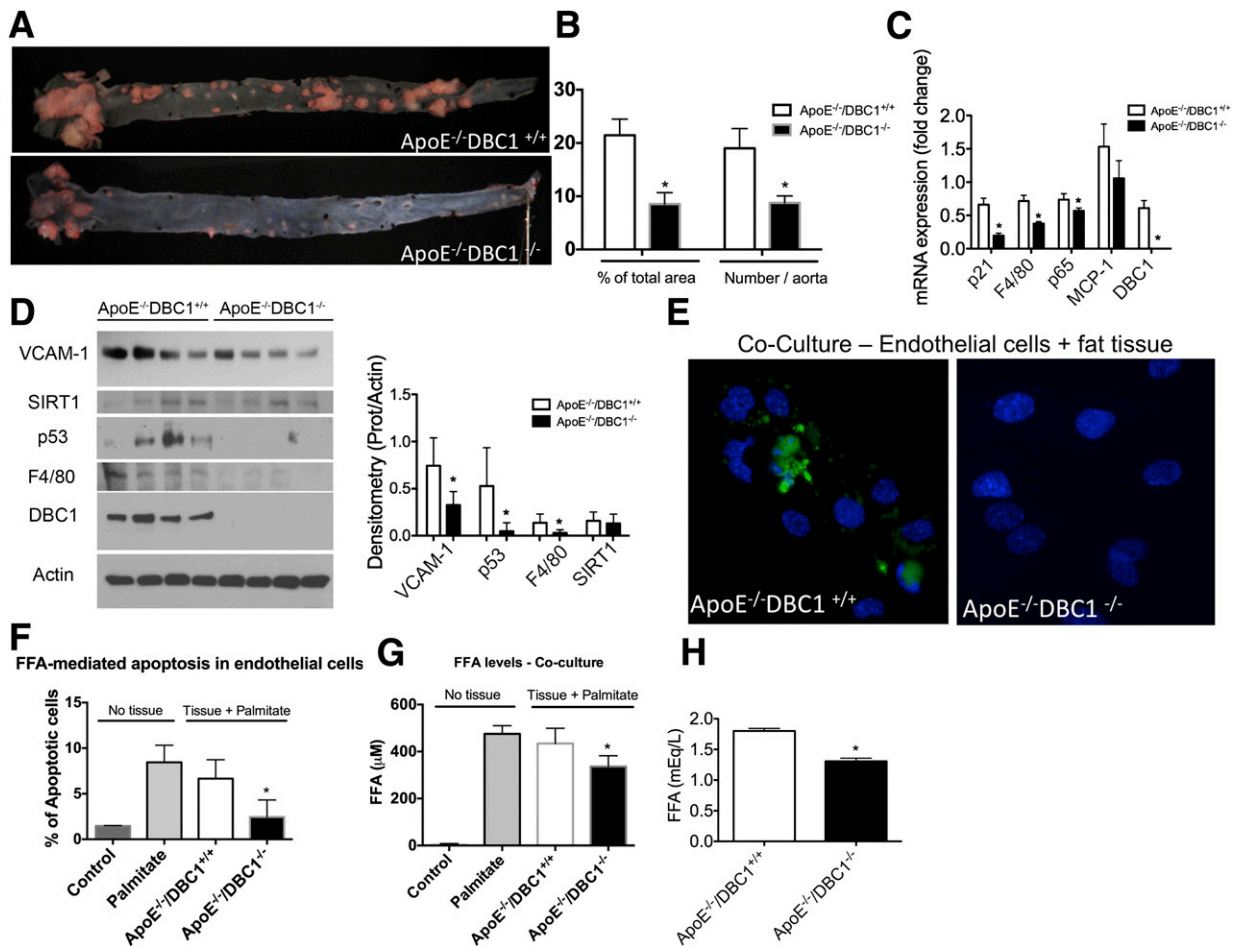


Figure 6—DBC1 KO protects against aortic atherosclerosis, inflammation, and cellular and tissue damage. **A**: Oil Red O staining of dissected aorta from ApoE^{-/-}/DBC1^{+/+} (upper panel) and ApoE^{-/-}/DBC1^{-/-} mice (lower panel) after 20 weeks of being fed the Western diet. **B**: Quantitation of the number of lesions and the total area with lesions described in **A** ($n = 5$ per group). *Shows significant difference at $P < 0.05$, t test. **C**: mRNA expression in whole aorta from ApoE^{-/-}/DBC1^{+/+} and ApoE^{-/-}/DBC1^{-/-} mice after 20 weeks of being fed the Western diet ($n = 5$ per group). *Shows significant difference at $P < 0.05$, t test. **D**: *Left*, Western blots from whole aortas dissected from ApoE^{-/-}/DBC1^{+/+} and ApoE^{-/-}/DBC1^{-/-} mice after 20 weeks of being fed the Western diet. *Right*, Quantitation of band intensity by densitometry ($n = 4$ per group). *Shows significant difference at $P < 0.05$, t test. **E**–**G**: Coculture of human aorta endothelial cells (HAEC) with ApoE^{-/-}/DBC1^{-/-} fat depot results in protection against palmitate-induced cellular apoptosis. Inguinal fat depots were dissected from ApoE^{-/-}/DBC1^{+/+} and ApoE^{-/-}/DBC1^{-/-} mice and incubated in media containing 500 $\mu\text{mol/L}$ sodium palmitate. HAEC were added to the media after 8 h, and cells and tissue were incubated together overnight. **E**: Representative image of caspase-3 activation (green label) after treatment with palmitate overnight in the presence of fat tissue. DAPI (blue label) was used for total cell number quantitation. **F**: The percentage of caspase-3-positive cells (i.e., apoptotic cells) in each condition was calculated by comparing the number of caspase-3-positive cells with the total number of cells. **G**: After the treatment, FFA levels in the media were measured ($n = 3$ per group). *Shows significant difference at $P < 0.05$, t test. **H**: FFA levels in plasma in ApoE^{-/-}/DBC1^{+/+} and ApoE^{-/-}/DBC1^{-/-} mice after 20 weeks of being fed the high-fat diet ($n = 8$ per group). *Shows significant difference at $P < 0.05$, t test.

In previous work we showed that DBC1 KO mice were protected against high-fat diet-induced liver steatosis by a molecular mechanism that involves SIRT1 activation in the liver (15). Our new findings suggest that protection against liver steatosis in the absence of DBC1 may be a consequence of intrinsic protection against fat deposition in the liver but also as a bystander effect of decreased FFA in plasma mediated by increased adipocyte storage capacity. Although we cannot rule out the possibility that other molecular targets of DBC1 besides SIRT1 are playing a role in the final phenotype observed, we found that DBC1 KO mice preserve SIRT1 activity during high-fat

diet-induced obesity. The role of SIRT1 in fat tissue development and function is still not completely clear. Some investigators have found that SIRT1 activation decreases body weight and fat tissue content (25,36), whereas others showed no significant effect in weight gain when mice were fed a high-fat diet (37). On the contrary, loss of function of SIRT1 decreases body weight and fat tissue content in mice fed a high-fat diet (38).

Regardless, whether the main molecular target of DBC1 in fat is SIRT1, we believe the DBC1 protein is part of a molecular switch that limits fat storage capacity, which in a chronic situation, will lead to fat tissue

damage, lipotoxicity, and peripheral tissue dysfunction. This will eventually lead to the development of type 2 diabetes, fatty liver disease, and cardiovascular diseases. Previous findings also support the idea that prevention of fatty acid spillover disconnects obesity from its deleterious effects. The transgenic mice that overexpress the hormone adiponectin on an *ob/ob* background show a similar phenotype as the DBC1 KO mice because they become more obese but preserve insulin sensitivity and show low levels of FFA in plasma (10). The antidiabetic drug rosiglitazone has metabolic effects that resemble the phenotype of DBC1 deletion. Rosiglitazone, a peroxisome proliferator-activated receptor- γ agonist, increases insulin sensitivity and lowers FFA levels and glycemia in animal models and in patients, although it also promotes weight gain through increased fat accumulation (39,40). Interestingly, it has been shown that DBC1 KO mice show phenotypic similarities with peroxisome proliferator-activated receptor- γ activation (41). Finally, mice that overexpress PEPCK specifically in fat tissue also show increased obesity due to fat accumulation but protection against insulin resistance (11). In agreement with this, we recently showed that DBC1 controls PEPCK expression by a mechanism that is dependent on SIRT1 (31). We found that DBC1 KO mice showed increased PEPCK expression in the liver, similar to what we show here for fat tissue, and as result of that, they have increased gluconeogenesis (31).

Our work brings a new insight into the link between obesity and metabolic diseases and provides a molecular mechanism that involves control of fat storage capacity and as a probable cause for the onset of metabolic syndrome. We propose that DBC1 acts as part of a molecular switch to stop fat accumulation in fat tissue, probably by regulating fat tissue inflammation, preadipocyte differentiation capacity, and also fatty acid esterification capacity in adipocytes. Pinpointing the exact molecular mechanism involved in the effect of DBC1 on fat tissue function is the goal of future work being conducted by our laboratory. Interestingly, the evolutionary role of an active molecular switch that prevents fat accumulation and leads to fatty acid spillover and the development of metabolic syndrome seems puzzling at first. However, we speculate that the main role of the DBC1-mediated fat tissue dysfunction and decrease in adipocyte storage capacity is to prevent the development of the “morbidly obese” phenotype that in the short-term would impair physical fitness in the wild. In contrast, the development of metabolic syndrome induced by the DBC1-mediated switch would cause health problems only much later in life.

In conclusion, there is growing evidence that supports the notion that obesity-driven metabolic diseases develop as a consequence of saturation of fat storage capacity in fat tissue. In the context of a high-caloric diet, obesity may act as a protective mechanism against diseases until fat tissue capacity is overloaded. Understanding the pathways that are involved in load capacity of fat tissue may provide new venues to treat obesity-driven metabolic

diseases. Our work establishes a molecular connection between fat load capacity in fat tissue and metabolic peripheral tissue damage. The relative contribution to the different pathways regulated by DBC1 to the overall phenotype found will be the subject of future investigation and may provide new ways for intervention against deleterious effects of obesity.

Acknowledgments. The authors thank Dr. Thomas A. White and Glenda Evans (Kogod Aging Center, Mayo Clinic, Rochester, MN) for technical assistance with microCT scan.

Funding. This work was supported mainly by National Institutes of Health (National Institute of Diabetes and Digestive and Kidney Diseases) grant DK-084055 (E.N.C.). Support was also from National Institutes of Health (National Institute on Aging) grants AG-41122 and AG-13925 (J.L.K.), American Heart Association Post-doctoral Fellowship 11POST7320060, and Agencia Nacional de Investigación e Innovación (DCI-ALA/2011/023-502 “Contrato de apoyo a las políticas de innovación y cohesión territorial”) (C.E.).

Duality of Interest. No potential conflicts of interest relevant to this article were reported.

Author Contributions. C.E. planned the experimental strategy and executed most of the experiments. V.N. participated in the *in vivo* experiments and quantified all of the atherosclerotic lesions. T.P. participated in culture and differentiation of preadipocytes and fat depot isolation. C.C.S.C. participated in cell culture experiments, insulin sensitivity (AKT phosphorylation), and strategy design. T.T. and J.L.K. provided expertise in the adipocyte tissue experiments. C.E., T.T., J.L.K., and E.N.C. wrote the manuscript. E.N.C. conceptualized the main hypothesis of the study, planned the experimental strategy, and performed fat tissue isolation and some *in vivo* insulin sensitivity assessments. E.N.C. is the guarantor of this work and, as such, had full access to all the data in the study and takes responsibility for the integrity of the data and the accuracy of the data analysis.

References

1. Flegal KM, Graubard BI, Williamson DF, Gail MH. Cause-specific excess deaths associated with underweight, overweight, and obesity. *JAMA* 2007;298:2028–2037
2. National Institutes of Health. *Strategic Plan for NIH Obesity Research*. Bethesda, MD, National Institutes of Health, 2004
3. Tchkonja T, Morbeck DE, Von Zglinicki T, et al. Fat tissue, aging, and cellular senescence. *Aging Cell* 2010;9:667–684
4. Unger RH, Scherer PE. Gluttony, sloth and the metabolic syndrome: a roadmap to lipotoxicity. *Trends Endocrinol Metab* 2010;21:345–352
5. Wang MY, Grayburn P, Chen S, Ravazzola M, Orci L, Unger RH. Adipogenic capacity and the susceptibility to type 2 diabetes and metabolic syndrome. *Proc Natl Acad Sci U S A* 2008;105:6139–6144
6. Listenberger LL, Han X, Lewis SE, et al. Triglyceride accumulation protects against fatty acid-induced lipotoxicity. *Proc Natl Acad Sci U S A* 2003;100:3077–3082
7. Almandoz JP, Singh E, Howell LA, et al. Spillover of Fatty acids during dietary fat storage in type 2 diabetes: relationship to body fat depots and effects of weight loss. *Diabetes* 2013;62:1897–1903
8. Asterholm IW, Halberg N, Scherer PE. Mouse models of lipodystrophy key reagents for the understanding of the metabolic syndrome. *Drug Discov Today Dis Models* 2007;4:17–24
9. Savage DB. Mouse models of inherited lipodystrophy. *Dis Model Mech* 2009;2:554–562
10. Kim JY, van de Wall E, Laplante M, et al. Obesity-associated improvements in metabolic profile through expansion of adipose tissue. *J Clin Invest* 2007;117:2621–2637

11. Franckhauser S, Muñoz S, Pujol A, et al. Increased fatty acid re-esterification by PEPCK overexpression in adipose tissue leads to obesity without insulin resistance. *Diabetes* 2002;51:624–630
12. Wildman RP. Healthy obesity. *Curr Opin Clin Nutr Metab Care* 2009;12:438–443
13. Naukkarinen J, Heinonen S, Hakkarainen A, et al. Characterising metabolically healthy obesity in weight-discordant monozygotic twins. *Diabetologia* 2014;57:167–176
14. Kim JE, Chen J, Lou Z. DBC1 is a negative regulator of SIRT1. *Nature* 2008;451:583–586
15. Escande C, Chini CC, Nin V, et al. Deleted in breast cancer-1 regulates SIRT1 activity and contributes to high-fat diet-induced liver steatosis in mice. *J Clin Invest* 2010;120:545–558
16. Zhao W, Kruse JP, Tang Y, Jung SY, Qin J, Gu W. Negative regulation of the deacetylase SIRT1 by DBC1. *Nature* 2008;451:587–590
17. Chini CC, Escande C, Nin V, Chini EN. HDAC3 is negatively regulated by the nuclear protein DBC1. *J Biol Chem* 2010;285:40830–40837
18. Chini CC, Escande C, Nin V, Chini EN. DBC1 (Deleted in Breast Cancer 1) modulates the stability and function of the nuclear receptor Rev-erb α . *Biochem J* 2013;451:453–461
19. Trauernicht AM, Kim SJ, Kim NH, Boyer TG. Modulation of estrogen receptor alpha protein level and survival function by DBC-1. *Mol Endocrinol* 2007;21:1526–1536
20. Koyama S, Wada-Hiraike O, Nakagawa S, et al. Repression of estrogen receptor beta function by putative tumor suppressor DBC1. *Biochem Biophys Res Commun* 2010;392:357–362
21. Hiraike H, Wada-Hiraike O, Nakagawa S, et al. Identification of DBC1 as a transcriptional repressor for BRCA1. *Br J Cancer* 2010;102:1061–1067
22. Li Z, Chen L, Kabra N, Wang C, Fang J, Chen J. Inhibition of SUV39H1 methyltransferase activity by DBC1. *J Biol Chem* 2009;284:10361–10366
23. Park SH, Riley P 4th, Frisch SM. Regulation of anoikis by deleted in breast cancer-1 (DBC1) through NF-kappaB. *Apoptosis* 2013;18:649–962
24. Vaughan M. The production and release of glycerol by adipose tissue incubated in vitro. *J Biol Chem* 1962;237:3354–3358
25. Chalkiadaki A, Guarente L. High-fat diet triggers inflammation-induced cleavage of SIRT1 in adipose tissue to promote metabolic dysfunction. *Cell Metab* 2012;16:180–188
26. Donkor J, Sparks LM, Xie H, Smith SR, Reue K. Adipose tissue lipin-1 expression is correlated with peroxisome proliferator-activated receptor alpha gene expression and insulin sensitivity in healthy young men. *J Clin Endocrinol Metab* 2008;93:233–239
27. Reue K. The role of lipin 1 in adipogenesis and lipid metabolism. *Novartis Found Symp* 2007;286:58–68; discussion 68–71, 162–163, 196–203
28. Ohman MK, Shen Y, Obimba CI, et al. Visceral adipose tissue inflammation accelerates atherosclerosis in apolipoprotein E-deficient mice. *Circulation* 2008;117:798–805
29. Öhman MK, Luo W, Wang H, et al. Perivascular visceral adipose tissue induces atherosclerosis in apolipoprotein E deficient mice. *Atherosclerosis* 2011;219:33–39
30. Chiba T, Nakazawa T, Yui K, Kaneko E, Shimokado K. VLDL induces adipocyte differentiation in ApoE-dependent manner. *Arterioscler Thromb Vasc Biol* 2003;23:1423–1429
31. Nin V, Chini CC, Escande C, Capellini V, Chini EN. Deleted in breast cancer 1 (DBC1) protein regulates hepatic gluconeogenesis. *J Biol Chem* 2014;289:5518–5527
32. Stancu CS, Toma L, Sima AV. Dual role of lipoproteins in endothelial cell dysfunction in atherosclerosis. *Cell Tissue Res* 2012;349:433–446
33. Lu Y, Qian L, Zhang Q, et al. Palmitate induces apoptosis in mouse aortic endothelial cells and endothelial dysfunction in mice fed high-calorie and high-cholesterol diets. *Life Sci* 2013;92:1165–1173
34. Appleton SL, Seaborn CJ, Visvanathan R, et al.; North West Adelaide Health Study Team. Diabetes and cardiovascular disease outcomes in the metabolically healthy obese phenotype: a cohort study. *Diabetes Care* 2013;36:2388–2394
35. Escande C, Nin V, Pirtskhalava T, et al. Deleted in Breast Cancer 1 regulates cellular senescence during obesity. *Aging Cell* 2014 July 3 [Epub ahead of print]
36. Bordone L, Cohen D, Robinson A, et al. SIRT1 transgenic mice show phenotypes resembling calorie restriction. *Aging Cell* 2007;6:759–767
37. Pfluger PT, Herranz D, Velasco-Miguel S, Serrano M, Tschöp MH. Sirt1 protects against high-fat diet-induced metabolic damage. *Proc Natl Acad Sci U S A* 2008;105:9793–9798
38. Caron AZ, He X, Mottawea W, et al. The SIRT1 deacetylase protects mice against the symptoms of metabolic syndrome. *FASEB J* 2014;28:1306–1316.
39. Hallakou S, Doaré L, Foufelle F, et al. Pioglitazone induces in vivo adipocyte differentiation in the obese Zucker fa/fa rat. *Diabetes* 1997;46:1393–1399
40. Miyazaki Y, Glass L, Triplitt C, et al. Effect of rosiglitazone on glucose and non-esterified fatty acid metabolism in Type II diabetic patients. *Diabetologia* 2001;44:2210–2219
41. Qiang L, Wang L, Kon N, et al. Brown remodeling of white adipose tissue by Sirt1-dependent deacetylation of Ppar γ . *Cell* 2012;150:620–632